Supporting information

A stretchable conductive elastomer sensor with self-healing and highly linear strain for human movement detection and pressure response

Yao Zhang, [a] *Yizhong Yuan,* *[a] *Huimei Yu,* *[b] *Chunhua Cai,* [c] *Jinyu Sun,* [a] *and Xiaohui Tian* [a]

a. School of Materials Science and Engineering, Shanghai Key Laboratory of Advanced Polymeric Materials, East China University of Science and Technology, Shanghai, 200237, P. R. China.
b. School of Materials Science and Engineering, East China University of Science and Technology, Shanghai, 200237, P. R. China.
c. Shanghai Key Laboratory of Advanced Polymeric Materials, Key Laboratory for Ultrafine Materials of Ministry of Education, Frontiers Science Center for Materiobiology and Dynamic Chemistry, School of Materials Science and Engineering, East China University of Science and Technology, Shanghai, 200237, P. R. China.

*Corresponding author: TEL: +86-21-18917102167; E-mail: yzhyuan@ecust.edu.cn.

*Corresponding author: TEL: +86-21-64252275; E-mail: huimeiyu@ecust.edu.cn.

EXPERIMENTAL SECTION

Materials.

Deproteinized natural rubber DPNR latex (DPNR, 60 wt% solid content) was provided by Hunan Vontex New Material Technology Co., Ltd. (China). Polyethylene glycol monododecyl ether (Brij-35), potassium persulfate (KPS, 99.5%), Isopropyl alcohol (IPA, ≥99.6%, AR), phytic acid solution (PA, 50 wt%), and ammonium persulfate (APS, AR) were purchased from Shanghai Macklin Biochemical Co., Ltd. (China). Hydrochloric acid (HCl, 36–38 wt%) was purchased from Sinopharm Chemical Reagent Co., Ltd. (China). Aniline (ANI, AR) was purchased from Shanghai Aladdin Bio-Chem Technology Co., Ltd. (China). Maleic anhydride (MA, AR) was purchased from Shanghai Adamas Reagent Co., Ltd. (China).

Preparation of MNR-PANI and MNR-PANI-PA compounds

First, 0.3 g isopropyl alcohol and 0.18 g Brij-35 were introduced in 10 g DPNR as stabilizers and emulsifiers, respectively. The mixture was stirred for 1 h in N_2 atmosphere at 25 °C. 2 mol/L HCl was added to acidify it to a pH of 4. Then, 0.3 g MA dissolved in 5g of water was added to the resulting DPNR latex. After that, the free radical initiator (0.15g KPS) was added at 70 °C and stirred for 6 h to obtain the MNR latex.

Second, the MNR latex was placed in an ice bath to keep it at 0-5 °C. Typically, 0.3 g ANI was dissolved in 10 g 20 wt% PA solution and stirred vigorously for 3 minutes to ensure adequate dissolution and protonation of ANI. The resulting ANI solution was added to the MNR latex and kept stirring for 1 h to ensure its uniform distribution in the latex. After that, the redox initiator APS aqueous solution (APS/ANI molar ratio of 1:1) was gradually dripped into the latex. The mixture reacted for 12 h in the temperature-controlled ice bath until ANI was fully polymerized. Finally, the mixture was poured into the polytetrafluoroethylene (PTFE) molds and dried at 50 °C for 12 h to obtain the MNR-PANI-PA compound film. Under the same experimental conditions, MNR-PANI-PA compound films with different PANI

contents were prepared. For the MNR-PANI compound film, ANI was dissolved in 1 mol/l HCl aqueous solution before being added to the MNR latex, and the corresponding amount of APS was added.

Structural and morphological characterization

FT-IR spectra with a wavenumber range between 400-4000 cm^{-1} were controlled by Bruker-VERTEX 80v (Germany). Test conditions of FT-IR spectra: 32 scans, 4 cm^{-1}, attenuated total reflectance (ATR). temperature-dependent FTIR spectra were performed on thermo fisher IS-50 (American). EDS scans were characterized by a field emission scanning electron microscope (S-4800, HITACHI, Japan) at an accelerating voltage of 10 kV. TEM was performed on transmission electron microscopy (JEM-2100, JEOL, Japan) at an accelerating voltage of 100 kV. The suspension was diluted to a concentration of approximately 0.5 wt % and stained with 2 wt % tungsten phosphate solution. XRD patterns were tested on an X-ray powder diffractometer (D/max2550VB, Rigaku, Japan).

Mechanical Properties

The tensile properties of materials were conducted in an electromechanical universal testing machine (LGD5000, Kunshan Lugong Precision Instrument Co. Ltd., China). The film was cut into a standard dumbbell shape. The rate of the uniaxial tensile test was 200 mm/min, and that of the cyclic tensile test was 80 mm/min.

Measurement of the Strain Sensor

The electrical conductivity σ was calculated by the following formula:

$$\sigma = \frac{L}{R \times A}$$

Where L is the length of the sample, R is the resistance of the sample measured by a precision resistance tester (CXT2515, Changzhou XY electronic Co., LTD., China), and A is the cross-sectional area of the sample.

The gauge factor (GF) can be used to measure the sensitivity of strain sensors and is defined as the ratio of relative resistance changes to the strain, indicating the degree of responsiveness to internal and external electronic changes.GF was calculated by the following formula:

$$GF = \frac{\Delta R/R_0}{\varepsilon} = \frac{|(R - R_0)|/R_0}{\varepsilon}$$

Where ε is the strain, R and R_0 represent the measured resistance and initial resistance, respectively.

The response signals about $\Delta R/R_0$ were obtained by using the coupled test system of the resistance tester and electromechanical universal testing machine.

The MNR-10PANI-PA film was cut into 60 mm × 7 mm rectangular strips to fabricate the strain sensor. Then copper sheets and wires were mounted at both sides of the above specimen to form a strain sensor. The sensors were secured to the skin of humans with the aid of medical tape. Volunteers signed an informed consent form for experiment-related information.

To fabricate the 4×4 sensing array, the MNR-10PANI-PA compound was cut into 4 uniform 1.5×1.5 cm square pieces and the conductive silver paste was uniformly applied to the insulating polyethylene terephthalate (PET) film. The relevant resistance signals are collected by the multi-channel resistance acquisition module.

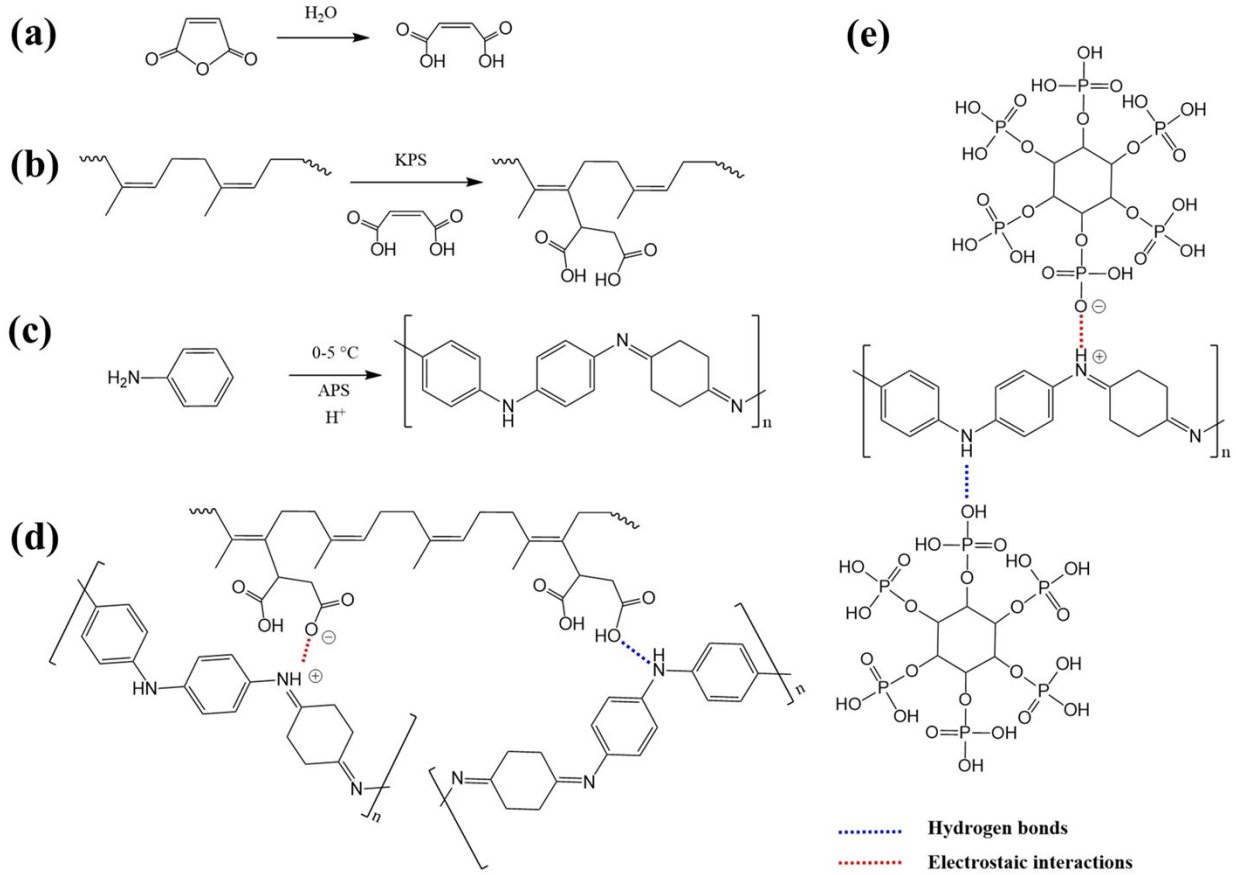

Scheme S1. (a) Maleic anhydride hydrolyzed to maleic acid. (b) The grafting of maleic acid onto the natural rubber. (c) Polymerization of PANI. (d-e) Non-covalent interaction between MNR, PANI, and PA.

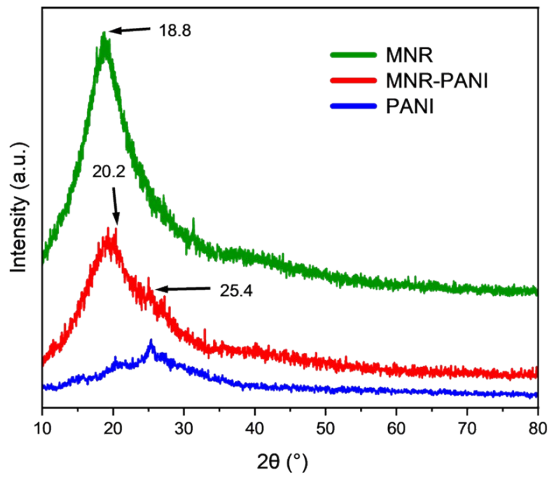

Figure S1. XRD patterns of MNR, MNR-PANI composite film, and pure PANI, respectively. The diffraction peaks at 2θ = 25.4° and 20.2° are crystalline peaks of pure PANI.[1] For MNR, there is only one amorphous peak at 18.8°, while characteristic diffraction peaks appear in the XRD pattern of MNR-PANI, indicating the regular arrangement of PANI in the material.

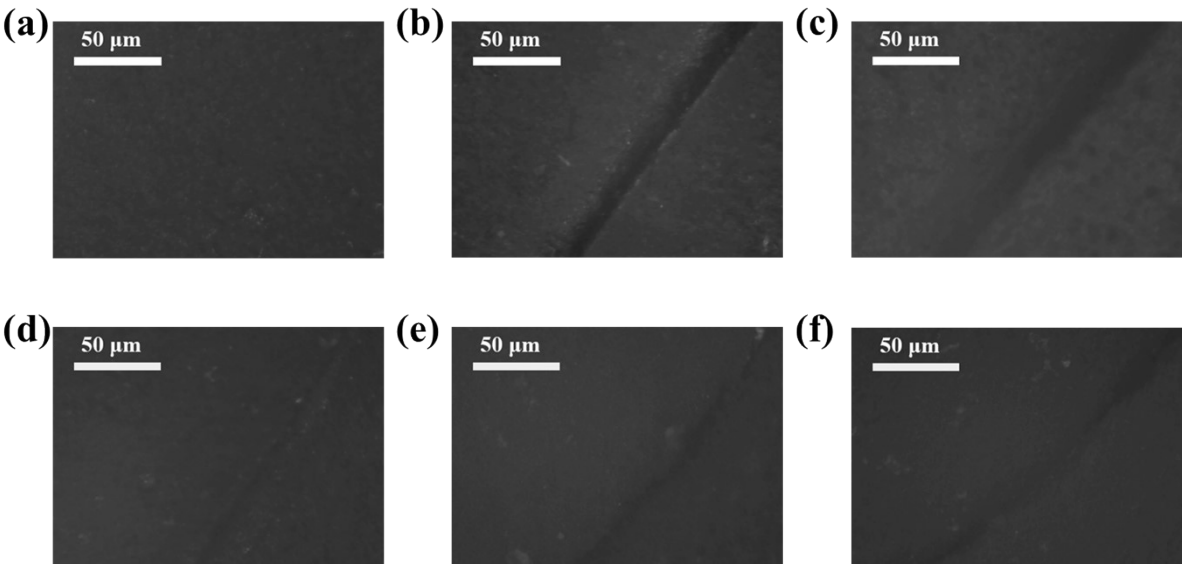

Figure S2. Optical microscopy images of MNR-10PANI-PA compounds film exhibiting the evolution of the cutting and healing process at 25 °C: (a) Original surface; (b) After the film is cut in half and bonded together along the section; (c) The cut surface was gently pressed for several seconds (3~5 s) to promote the self-healing; (d) After about 10 min of self-healing; (e) After 50% strain stretching; (f) After 100% strain stretching.

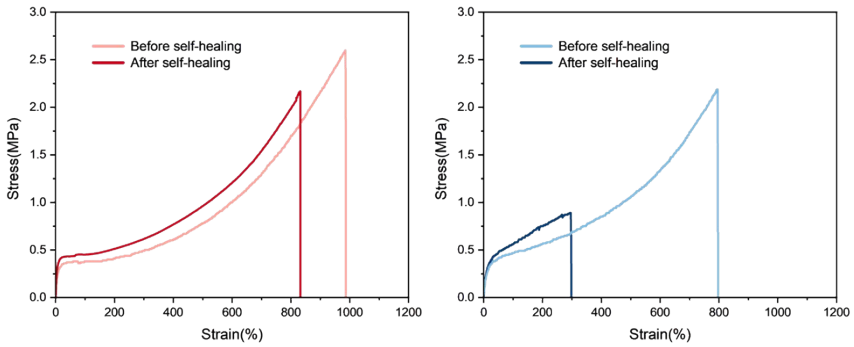

Figure S3. Stress−strain curves of MNR-10PANI films before and after self-healing with PA (a) and HCl(b).

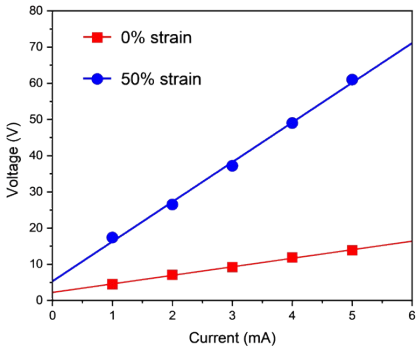

Figure S4. The voltage-current curves of MNR-10PANI-PA compounds under 0% and 50% strains.

Table S1. The comparison of this work with recently reported flexible conductive sensors in terms of mechanical properties, linearity, and self-healing ability.

Materials	Max stress (MPa)	Max strain (%)	Linearity			Self-healable	Reference
			Linear or not	Slope or GF	Strain (%)		
NR/GF	1.1	60	NO	210	40	NO	[2]
Graphene ink/PDMS	/	/	YES	/	0-15	NO	[3]
			NO	1054	26		
CNT/PS	/	800	NO	0.65	400	NO	[4]
				48	700		
AgNWs/PDMS	/	70	YES	5	0-50	NO	[5]
GWF/PDMS	/	8	NO	10^3	6	NO	[6]
				10^6	8		
PVA/PAA/CMC/AgNWs	0.06	2975	NO	0.53	150	YES	[7]
				1.14	600		
				4.59	750		
PEDOT: PSS/PU/SWCNT	/	100	NO	62.7	100	NO	[8]
AgNWs/PAAM/PVP	0.05	22000	YES	0.21	0-1000	YES	[9]
			YES	0.71	100-18100		
AgNWs/PEDOT:PSS/PDMS	/	/	YES	8.55	0-20	NO	[10]
			YES	2.35	20-100		
PDMS/AgNPs/PPy/NS	0.4	70	YES	33.8	0-30	NO	[11]
			NO	1610	70		
PDMS/PPy/PU	0.88	652	NO	1251	130	YES	[12]
PANI/PAA/PA	1.6	460	YES	11.6	0-100	YES	[13]
			YES	4.7	100-460		
PAAMPSA/PANI/PA	0.4	1935	NO	/	/	YES	[14]
PVA/PANI/Glycerin	0.5	500	YES	2.14	0-100	NO	[15]
PANI/PVA-CBA	4.35	380	NO	2.18	300	YES	[16]
PANI/P(PEG-co-AA)	0.6	1000	YES	2.43	0-200	YES	[17]
PANI/PAAM/AA)/Fe^{3+}	0.21	442	YES	0.48	0-400	NO	[18]
MNR-PANI-PA	2.5	1000	YES	13.84	0-250	YES	This work
				32.01	250-1000		

Abbreviations:

NR: Natural rubber. GF: Graphene foam. PDMS: Polydimethylsiloxane. CNT: Carbon nanotubes. PS: Polystyrene. AgNWs: Silver nanowires. GWF: Graphene woven fabrics. PVA: Polyvinyl alcohol. PAA: Polyacrylic acid. CMC: Carboxymethyl cellulose. SWCNTs: Single-wall carbon nanotubes. PEDOT:PSS: Poly(3,4-ethylenedioxythiophene) polystyrenesulfonate. PAAM: Polyacrylamide. PVP: polyvinylpyrrolidone. PPy: polypyrrole. AgNPs: Ag nanoparticles. NS: Nylon strip. PANI: Polyaniline. PA: Phytic acid. PAAMPSA: Poly(2-acrylamido-2-methyl1-propanesulfonic acid). CBA: 4-carboxybenzaldehyde. P(PEG-co-AA): Poly [poly (ethylene glycol) methacrylate-co-acrylic acid (AA)]

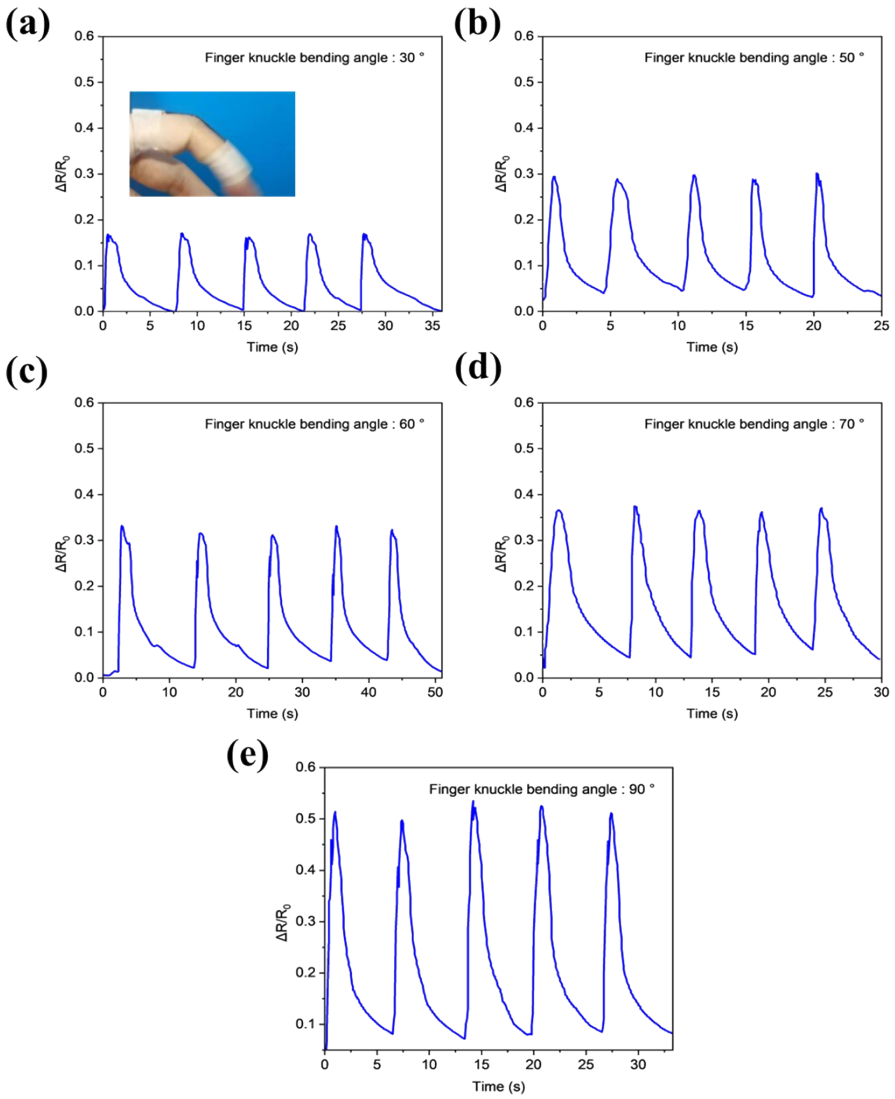

Figure S5. ΔR/R0 signal curves of different finger knuckle bending angles: (a) 30°, (b) 50°, (c) 60°, (d) 70°, and (e) 90°.

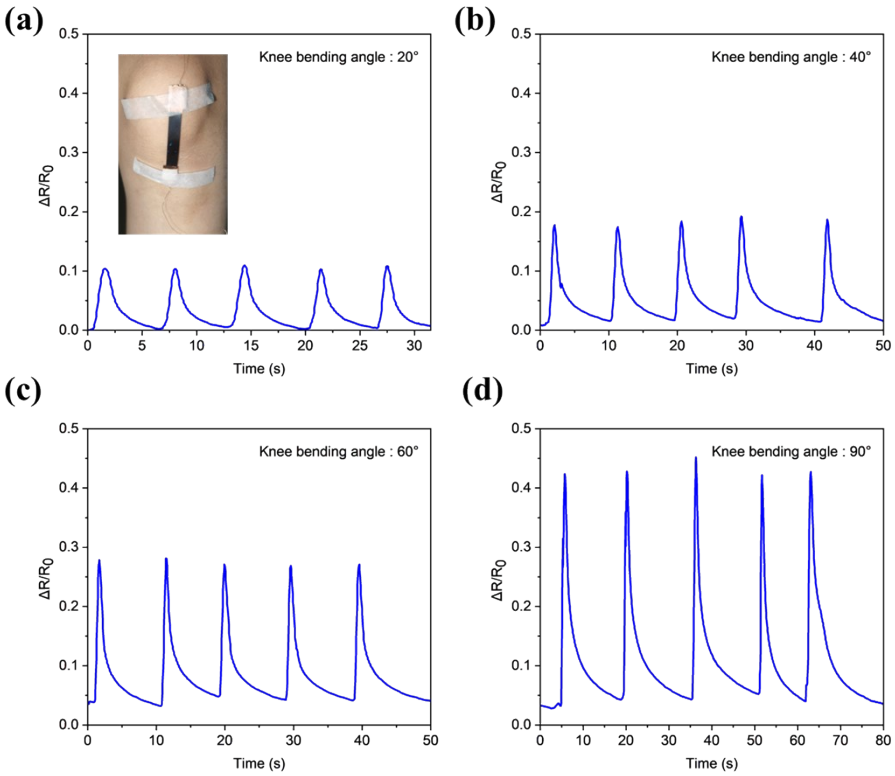

Figure S6. ΔR/R0 signal curves of different knee bending angles: (a) 20°, (b) 40°, (c) 60°, and (d) 90°.

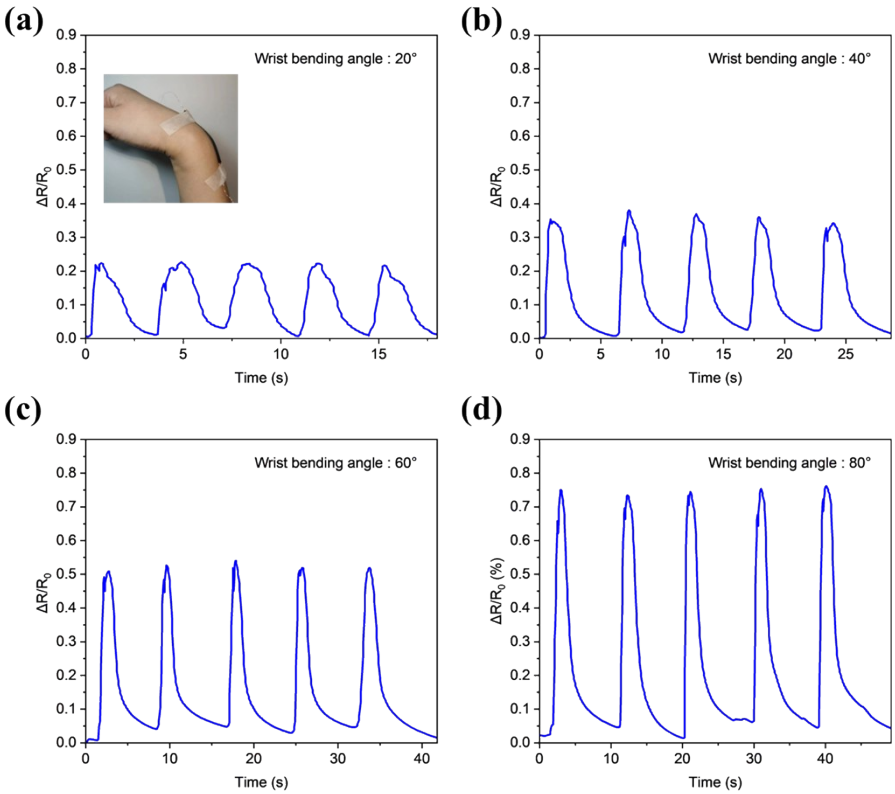

Figure S7. ΔR/R0 signal curves of different wrist bending angles: (a) 20°, (b) 40°, (c) 60°, and (d) 80°.

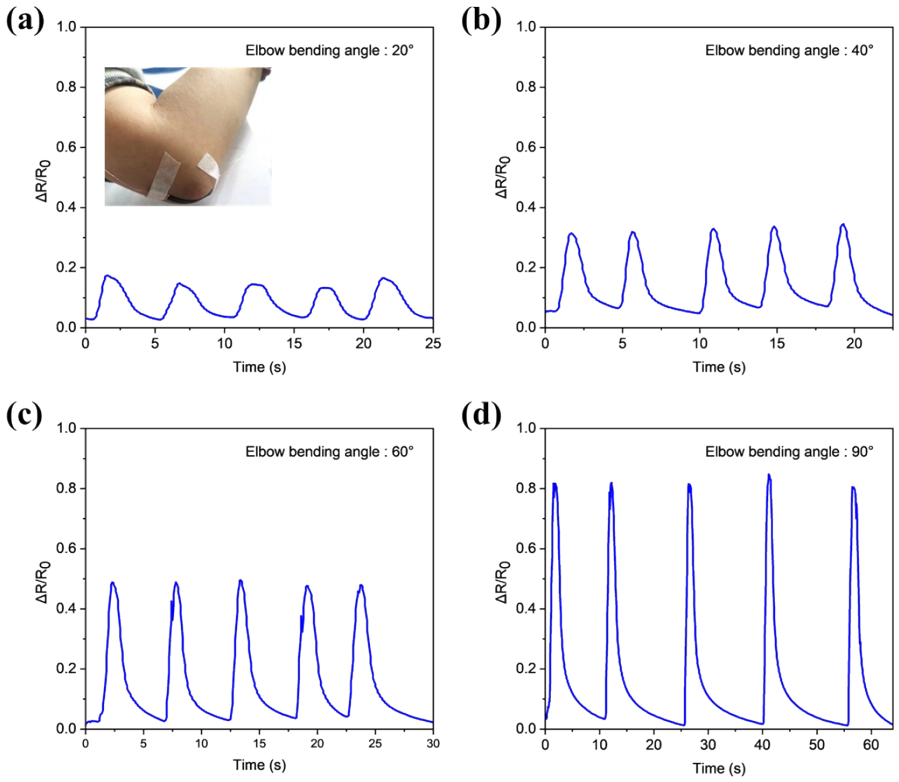

Figure S8. ΔR/R0 signal curves of different elbow bending angles: (a) 20°, (b) 40°, (c) 60°, and (d) 90°.

Reference

1. J. Yan, T. Wei, B. Shao, Z. Fan, W. Qian, M. Zhang and F. Wei, *Carbon*, 2010, **48**, 487-493.
2. W. Zhang, B. Yin, J. Wang, A. Mohamed and H. Jia, *Journal of Alloys and Compounds*, 2019, **785**, 1001-1008.
3. Y. F. Yang, L. Q. Tao, Y. Pang, H. Tian, Z. Y. Ju, X. M. Wu, Y. Yang and T. L. Ren, *Nanoscale*, 2018, **10**, 11524-11530.
4. S. J. Park, J. Kim, M. Chu and M. Khine, *Advanced Materials Technologies*, 2016, **1**, 1600053.
5. M. Amjadi, A. Pichitpajongkit, S. Lee, S. Ryu and I. Park, *Acs Nano*, 2014, **8**, 5154-5163.
6. X. Li, R. Zhang, W. Yu, K. Wang, J. Wei, D. Wu, A. Cao, Z. Li, Y. Cheng, Q. Zheng, R. S. Ruoff and H. Zhu, *Sci Rep*, 2012, **2**, 870.
7. W. Zhao, X. Qu, Q. Xu, Y. Lu, W. Yuan, W. Wang, Q. Wang, W. Huang and X. Dong, *Advanced Electronic Materials*, 2020, **6**, 2000267.
8. E. Roh, B. U. Hwang, D. Kim, B. Y. Kim and N. E. Lee, *Acs Nano*, 2015, **9**, 6252-6261.
9. H. Zhang, W. Niu and S. Zhang, *ACS Appl Mater Interfaces*, 2019, **11**, 24639-24647.
10. G. Z. Shen, B. H. Chen, T. L. Liang, Z. H. Liu, S. R. Zhao, J. Y. Liu, C. Zhang, W. J. Yang, Y. L. Wang and X. He, *Advanced Electronic Materials*, 2020, **6**, 1901360.
11. J. Peng, B. Wang, H. A. Cheng, R. H. Yang, Y. J. Yin, S. Xu and C. X. Wang, *Composites Science and Technology*, 2022, **227**, 109561.

12. Y. F. Shan, Z. X. Li, T. W. Yu, X. X. Wang, H. Cui, K. Yang and Y. Y. Cui, *Composites Science and Technology*, 2022, **218**, 109208.
13. T. Wang, Y. Zhang, Q. Liu, W. Cheng, X. Wang, L. Pan, B. Xu and H. Xu, *Advanced Functional Materials*, 2017, **28**, 1705551.
14. Y. Lu, Z. Liu, H. Yan, Q. Peng, R. Wang, M. E. Barkey, J. W. Jeon and E. K. Wujcik, *ACS Appl Mater Interfaces*, 2019, **11**, 20453-20464.
15. C. Hu, Y. Zhang, X. Wang, L. Xing, L. Shi and R. Ran, *ACS Appl Mater Interfaces*, 2018, **10**, 44000-44010.
16. X. Wang, L. Weng, X. Zhang, L. Guan and X. Li, *Journal of Science: Advanced Materials and Devices*, 2023, **8**, 100563.
17. X. Yu, H. Zhang, Y. Wang, X. Fan, Z. Li, X. Zhang and T. Liu, *Advanced Functional Materials*, 2022, **32**, 2204366.
18. X. Sun, H. Wang, Y. Ding, Y. Yao, Y. Liu and J. Tang, *J Mater Chem B*, 2022, **10**, 1442-1452.